Check for upd

JAWRA Journal of the American Water Resources Association

SPECIAL ISSUE Water Reclamation and Reuse in a Changing World

RESEARCH ARTICLE

Economic Loss Assessment of Water Supply–Demand Imbalance in the Yellow River Basin Under Low-Flow Scenarios

Wenxiu Shang[1] | Juan Jing[1] | Yifan Wei[2] | Haodong Deng[1] | Hong Lv[1] | Xiaokang Zheng[1]

[1]Yellow River Engineering Consulting Co., Ltd., Zhengzhou, China | [2]Lingxi College, Dalian University of Technology, Dalian, Liaoning, China

Correspondence: Haodong Deng (13253610702@163.com)

Received: 10 July 2026 | **Revised:** 30 August 2026 | **Accepted:** 25 September 2026

Keywords: economic loss assessment | low-flow scenario | Monte Carlo simulation | risk loss integral model | water supply–demand imbalance | Yellow River Basin

ABSTRACT

Low-flow events trigger water-supply shortages and supply–demand imbalances in water-scarce developed basins; assessing their economic losses informs water-security risk identification and water-resources regulation. This paper establishes an economic loss assessment framework integrating water supply variability, water demand constraints, and sectoral disparities. Combining a risk loss integral model with Monte Carlo simulation, it quantifies water shortage economic impacts across agriculture, industry, domestic and ecological sectors for China's Yellow River Basin. Scenarios covering typical low flow years, prolonged low flow periods, and multi-source regulation are constructed for 2022 (baseline) and 2035 (planned) to analyze spatiotemporal loss patterns and mitigation performance. Economic losses rise with low flow severity and spread toward the middle upper reaches. Basin-wide losses reach 74.66–574.82 × 10^8 CNY for 2022 and 264.11–730.19 × 10^8 CNY for 2035 across 75%, 90%, and 95% inflow frequency scenarios. Losses accumulate markedly during sustained low flow episodes, mainly hitting Inner Mongolia, Ningxia, Gansu and Shaanxi. Supplementary water measures mitigate losses; combined schemes outperform single interventions, yet marginal benefits decline with increasing water supply volumes. Losses are co-determined by local water endowment, water use structure, alternative water capacity and regulation policies.

1 | Introduction

Global climate change and human activities have jointly altered basin-scale hydrological processes, leading to more pronounced interannual variability in precipitation, runoff, and available water supply (Yang et al. 2022; Jiang et al. 2021). As a result, hydrological anomalies such as droughts and low-flow events have exerted increasing pressure on regional water resources systems (Dai 2013; Trenberth et al. 2014). Hydrological low-flow conditions are generally characterized by sustained below-normal streamflow, groundwater levels, or reservoir storage. Their development is influenced not only by meteorological drought, but also by underlying surface conditions, basin regulation capacity, and human water withdrawal activities (Mishra and Singh 2010; Van Loon 2015). In regions with intensive water resources development and utilization, low-flow processes directly reduce available water supply and further amplify the risk of water supply–demand imbalance by lowering water-supply reliability, intensifying competition among water-use sectors, and increasing the pressure on water resources regulation (Vörösmarty et al. 2000; Haddeland et al. 2014). At the global scale, water scarcity has become a major constraint on socioeconomic development and ecological security, while population growth, urban expansion, and increasing industrial water demand have further intensified conflicts between water supply and demand (Mekonnen and Hoekstra 2016; Liu et al. 2017). Therefore, assessing water supply–demand imbalance and its associated economic losses under low-flow scenarios is essential

© 2026 American Water Resources Association.

All rights reserved, including rights for text and data mining and training of artificial intelligence technologies or similar technologies.

for identifying basin water-security risks and supporting water resources regulation decisions.

The identification and assessment of low-flow events constitute an important component of water resources risk research. Existing studies have widely applied standardized drought and streamflow indices, threshold-based methods, and multi-index approaches to identify drought and low-flow events and characterize their duration, severity, and temporal evolution (Mukama et al. 2025; Wu et al. 2026). Recent studies have increasingly emphasized the propagation of drought across meteorological, hydrological, agricultural, ecological, and socioeconomic systems, with particular attention to the cascading effects of water deficits and their implications for water resources and socioeconomic activities (Zhen et al. 2025; Li et al. 2026). Previous studies have shown that the impacts of low-flow events are not determined solely by the degree of runoff reduction, but are also jointly constrained by reservoir regulation, water withdrawal behavior, demand rigidity, and regional adaptive capacity (Van Loon et al. 2016; Di Baldassarre et al. 2018). In water resources system assessment, indicators such as reliability, resilience, and vulnerability have often been used to evaluate system performance under adverse hydrological conditions (Hashimoto et al. 1982). In addition, Monte Carlo simulation and uncertainty analysis have been widely applied to characterize uncertainties in hydrological inputs, model parameters, and water-supply processes, thereby providing methodological support for risk-based water resources assessment (Beven and Binley 1992; Kuczera and Parent 1998).

Considerable research has been conducted on water scarcity and water supply–demand imbalance from the perspectives of water resources carrying capacity, water security, water-use efficiency, and supply–demand balance (Hoekstra et al. 2012; Hanasaki et al. 2013). Some studies have further incorporated climate change and socioeconomic development scenarios to assess future water scarcity risks and the potential effectiveness of adaptation measures (Schewe et al. 2014; Wanders and Wada 2015). At basin and regional scales, the impacts of water supply–demand imbalance are not merely reflected in water quantity deficits. Instead, they can be transformed into economic losses through multiple pathways, including agricultural yield reduction, restricted industrial output, increased pressure on domestic water supply, and degradation of ecosystem services (Flörke et al. 2018; Stahl et al. 2016). Existing studies on economic loss assessment have commonly emphasized the distinctions among direct losses, indirect losses, and non-market losses, and have highlighted substantial differences in the sensitivity of different sectors to water-shortage shocks (Fleming-Muñoz et al. 2023; Yang et al. 2023; Logar and van den Bergh 2013). Accordingly, economic loss assessment of water supply–demand imbalance under low-flow scenarios should jointly consider hydrological constraints, demand structure, sectoral differences, and regional economic exposure.

Against this broader research background, the Yellow River Basin is a typical water-scarce basin in China and serves as a strategic region supporting food production, energy development, urban growth, and ecological security in northern China. Under the combined effects of climate change and human activities, runoff processes in the Yellow River Basin exhibit significant spatial–temporal variability and stage-dependent changes. Declining natural runoff, increasing water demand, and constraints imposed by the water-source structure have jointly intensified water supply–demand conflicts in the basin (Miao et al. 2012). Previous studies have indicated that runoff changes in the Yellow River Basin are affected not only by climatic factors, but also by human activities such as irrigation withdrawal, reservoir operation, land-use change, and industrial development (Piao et al. 2010; Wang et al. 2013). Under conditions of intensive water resources development and utilization, water allocation in the Yellow River Basin must satisfy agricultural, industrial, and domestic water demands while also maintaining in-stream ecological water requirements and ecosystem stability (Cai et al. 2004). Therefore, when low-flow scenarios reduce available water supply, the exposure to water shortage, alternative water-supply capacity, and economic loss levels may vary substantially across regions and water-use sectors.

Although previous studies have provided important foundations for low-flow identification, water scarcity evaluation, and economic loss accounting, further research is still needed to quantitatively assess the economic losses caused by water supply–demand imbalance under low-flow scenarios in the Yellow River Basin. First, many existing studies have focused primarily on hydrological processes or water-supply reliability, while the quantitative characterization of how water supply–demand imbalance is transmitted to the economic system remains insufficient (AghaKouchak et al. 2021). Second, some studies still estimate losses using deterministic water deficits or a single water-price parameter, which makes it difficult to reflect the effects of water-supply uncertainty and sector-specific water-use values on loss outcomes (Freire-González et al. 2017; Jenkins et al. 2021). Third, the spatial heterogeneity of losses across provinces, the cumulative effects during consecutive low-flow periods, and the differences in loss reduction among multiple regulation schemes still need to be further identified in relation to the actual supply–demand structure of the basin (Mortazavi-Naeini et al. 2019; Salmoral et al. 2019). Therefore, it is necessary to develop an economic loss assessment framework for water supply–demand imbalance that is applicable to low-flow scenarios in the Yellow River Basin, and to reveal the spatio-temporal heterogeneity of economic losses and their responses to regulation measures under different low-flow conditions.

More importantly, existing deterministic loss-accounting approaches generally associate a prescribed water deficit with a single loss estimate, whereas the variability of realized water supply within a given low-flow condition is rarely incorporated directly into the economic-loss calculation. Therefore, an assessment framework is needed that links the probability of alternative water-supply states with sector-specific loss consequences under consistent low-flow scenarios.

Against this background, this study assesses the economic losses caused by water supply–demand imbalance under low-flow scenarios in the Yellow River Basin. First, the transmission mechanisms through which insufficient water supply leads to economic losses are analyzed from the perspectives of agricultural, industrial, domestic, and ecological water-use sectors. Second, a risk-loss framework is developed to integrate the probability of alternative water-supply states with sector-specific

shortage losses under a fixed demand scenario, while Monte Carlo simulation is used as the numerical tool for estimating the expected loss. This differs from deterministic shortage-loss accounting, which produces a single loss estimate for a prescribed water-deficit state. Finally, under current conditions in 2022 and planned conditions in 2035, typical low-flow years, consecutive low-flow periods, and multi-scheme regulation scenarios are established to evaluate the spatial distribution, temporal evolution, and loss-reduction effects of water supply–demand imbalance in the Yellow River Basin. The results are expected to provide quantitative support for low-flow risk identification, optimal water resources allocation, and coordinated multi-source water regulation in the Yellow River Basin.

2 | Study Area and Data

2.1 | Study Area

The Yellow River Basin is located in northern China, extending from the Bayan Har Mountains in the west to the Bohai Sea in the east, with a total drainage area of approximately 795,000 km^2 (Figure 1). The basin generally slopes from west to east and spans the Qinghai–Tibet Plateau, the Inner Mongolia Plateau, the Loess Plateau, and the Huang–Huai–Hai Plain, resulting in complex topography, geomorphology, and underlying surface conditions. The basin is mainly characterized by a temperate continental monsoon climate, with uneven spatial and temporal precipitation distribution. The Yellow River Basin is mainly characterized by a temperate continental monsoon climate, with uneven spatial and temporal precipitation distribution. More than 60% of the annual precipitation occurs from June to September, resulting in pronounced seasonal variations in basin hydrological conditions (Hu et al. 2025). The main stem of the Yellow River is approximately 5464 km long and represents one of the most important strategic water sources in northern China.

The Yellow River Basin is also an important grain-producing region, energy base, and ecological barrier. However, it is characterized by limited water resources endowment, low per capita water availability, and a high degree of water resources development and utilization, resulting in long-standing conflicts between water supply and demand. Climate change and human activities have substantially altered runoff processes in the Yellow River Basin (Wang, Li, et al. 2025; Wang, Zheng, et al. 2025). Three prolonged low-flow periods have been identified during 1922–1932, 1969–1974, and 1990–2002, with 2002 representing a particularly severe low-flow year (Yang et al. 2026). The combined effects of declining inflow and intensive water demand have exposed the Yellow River Basin to higher water-supply risks and greater economic exposure under severe low-flow conditions. Accordingly, this study selects the Yellow River Basin as the study area and evaluates the economic loss characteristics of water supply–demand imbalance under typical low-flow years, consecutive low-flow periods, and low-flow-year regulation scenarios under the current conditions in 2022 and the planned conditions in 2035.

2.2 | Data Sources

The data used in this study include socioeconomic statistics, basin-scale water supply and use data, and planned water demand. Socioeconomic data were obtained from provincial and prefecture-level statistical yearbooks in the Yellow River Basin and the China Rural Statistical Yearbook, and were used to characterize regional development and determine sector-specific economic water values. Water supply and use data for 1988–2022 were obtained from the Yellow River Water Resources Bulletin, including water supply by source and water use by sector. These publicly available data can be accessed through the National Bureau of Statistics of China and the Yellow River Conservancy Commission, respectively. Planned water demand for 2035 was obtained from the Demonstration Report of the Western Route of the South-to-North Water Diversion Project and was used to construct the planned demand scenario.

2.3 | Scenario Design

To assess the economic losses caused by water supply–demand imbalance in the Yellow River Basin under different low-flow conditions, this study constructs a scenario system from both the water demand and water supply perspectives. On the demand side, two scenarios are established: the current year condition in

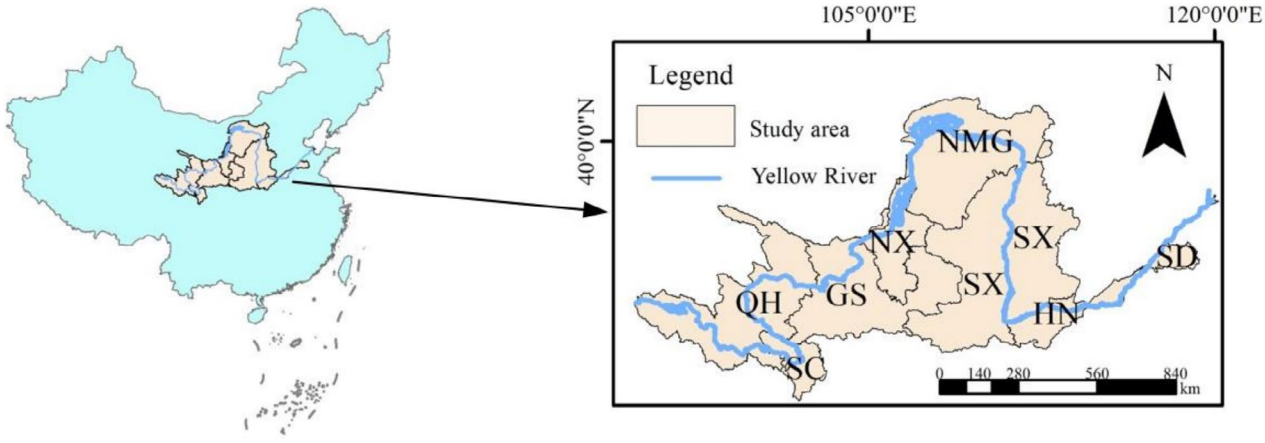

FIGURE 1 | Location of the study area.

2022 and the planned year condition in 2035, representing water demand levels at different stages of development. On the supply side, three types of scenarios are established: typical low-flow years, consecutive low-flow periods, and regulation schemes for a severe low-flow year. These scenarios are used to characterize water-supply constraints under different temporal scales and regulation conditions. Based on these scenario combinations, a comparative assessment of economic losses caused by water supply–demand imbalance in the Yellow River Basin is further conducted.

2.3.1 | Water Demand Scenarios

1. Current condition in 2022

The actual water use of the Yellow River Basin in 2022 is used as the current water-demand scenario. In 2022, the total water use was $409.4\times10^8\,m^3$ (Table 1). Agricultural water use accounted for approximately 64.7% of the total, followed by domestic (13.7%), ecological (11.2%), and industrial water use (10.4%). Surface water was the dominant supply source, accounting for approximately 68.3% of the total water supply.

2. Planned condition in 2035

The total water demand of the Yellow River Basin in 2035 is projected to reach $510.66\times10^8\,m^3$ (Table 2). Agricultural water demand remains the largest component, reaching $322.86\times10^8\,m^3$ and accounting for 63.2% of the total, although its proportion is lower than that in 2022. Domestic water demand is projected to reach $79.97\times10^8\,m^3$, accounting for 15.7%; industrial water demand is $69.42\times10^8\,m^3$, accounting for 13.6%; and ecological water demand is $38.41\times10^8\,m^3$, accounting for 7.5%.

2.3.2 | Water Supply Scenarios

The water supply scenarios are constructed based on the current water supply structure and designed with reference to previous studies on multi-source water-supply enhancement and regulation in the Yellow River Basin during severe low-flow years (Wang, Li, et al. 2025; Wang, Zheng, et al. 2025). These scenarios account not only for the constraints imposed by different inflow frequencies and consecutive low-flow processes on basin-scale available water supply, but also for the improvements in water-supply capacity resulting from regulation measures such as additional groundwater supply, water supplementation from the Eastern and Central Routes of the South-to-North Water Diversion Project, supplementation from the Longyangxia Reservoir, and in-channel water supplementation. Accordingly, three types of water supply scenarios are established in this study: typical low-flow year scenarios, consecutive low-flow period scenarios, and multi-scheme regulation scenarios for a severe low-flow year.

1. Typical low-flow year scenarios

Based on the current water-supply structure, typical low-flow year scenarios with inflow frequencies of 75%, 90%, and 95%

TABLE 1 | Water supply and water use in the Yellow River Basin in 2022 (unit: $10^8\,m^3$).

Region	Water use by sector					Water supply by source				
	Domestic	Industrial	Agricultural	Ecological	Total	Surface water	Groundwater	Non-conventional water	Transferred water	Total
QH	2.30	0.70	9.36	1.24	13.60	11.18	1.82	0.60	0.00	13.60
SC	0.14	0.01	0.19	0.00	0.34	0.32	0.01	0.00	0.00	0.33
GS	6.77	3.59	24.10	3.45	37.91	32.86	3.03	2.01	0.00	37.90
NX	3.70	4.46	53.64	4.53	66.33	60.08	4.93	1.33	0.00	66.34
NMG	5.45	9.26	72.55	21.86	109.12	79.25	25.45	4.43	0.00	109.13
SX	16.49	9.32	37.72	5.98	69.51	36.69	26.86	5.20	0.76	69.51
SAX	10.14	7.42	27.16	3.35	48.07	25.39	18.23	4.4	0.05	48.07
HN	8.13	5.31	29.61	4.14	47.19	25.37	19.48	1.93	0.41	47.19
SD	2.90	2.67	10.46	1.30	17.33	8.37	7.16	1.80	0.00	17.33
Basin	56.02	42.74	264.79	45.85	409.40	279.51	106.97	21.70	1.22	409.40

were established to represent progressively severe low-flow conditions. These scenarios were used to assess changes in basin water-supply capacity and the resulting economic losses from water supply–demand imbalance. For each scenario, available water supply was determined following the basin-scale allocation framework of Wang, Li, et al. (2025); Wang, Zheng, et al. (2025), rather than by proportional runoff scaling. Surface-water supply was then allocated among provinces according to the existing regional allocation structure, while other water sources followed the corresponding scenario assumptions.

2. Consecutive low-flow period scenario

The period 1990–2002 was selected because it represents a prolonged low-flow episode in the Yellow River Basin, during which natural runoff was approximately 20% below the long-term average (Yang et al. 2026). This period was used to simulate the cumulative pressure of persistent low inflow on the basin water-supply system and its associated economic losses.

3. Multi-scheme regulation scenarios for a severe low-flow year

The year 2002 was selected as a representative severe low-flow year because natural runoff was approximately 47% below the long-term average (Yang et al. 2026). Under this condition, single and combined supplementary water-supply measures were established to compare their loss-reduction effects.

The regulation scales in Table 3 were determined with reference to the feasible water-supply augmentation ranges and regulation schemes reported by Wang, Li, et al. (2025); Wang, Zheng, et al. (2025) for the Yellow River Basin under severe low-flow conditions. Based on the available capacities of groundwater supplementation, inter-basin water diversion, and reservoir regulation, representative low, medium, and high supplementation levels were selected to characterize different regulation intensities. Accordingly, groundwater supplementation was set at 10 and $20\times10^8\,m^3$, Longyangxia Reservoir supplementation at 10, 30, and $50\times10^8\,m^3$, and in-channel supplementation at 10 and $20\times10^8\,m^3$.

TABLE 2 | Water demand in the Yellow River Basin in 2035 (unit: $10^8\,m^3$).

Basin	Domestic	Industrial	Agricultural	Ecological	Total
Water demand	79.97	69.42	322.86	38.41	510.66
Share	15.7%	13.6%	63.2%	7.5%	100%

TABLE 3 | Low-flow encounter and water-supply regulation scenarios (unit: $10^8\,m^3$).

		Water demand	Groundwater		E–C Route	Longyangxia Reservoir			In-channel	
Scheme set		**409.4**	**10**	**20**	**6.2**	**10**	**30**	**50**	**10**	**20**
Baseline scheme	A0	√								
Single-measure scheme	A1-G1	√	√							
	A1-G2	√		√						
	A1-D	√			√					
	A1-R1	√				√				
	A1-R3	√					√			
	A1-R3-1	√					√		√	
	A1-R5	√						√		
	A1-R5-1	√						√	√	
	A1-R5-2	√						√		√
Combined-measure scheme	A2-GDR1	√		√	√	√				
	A2-GDR3	√		√	√		√			
	A2-GDR3-1	√		√	√		√		√	
	A2-GDR5	√		√	√			√		
	A2-GDR5-1	√		√	√			√	√	
	A2-GDR5-2	√		√	√			√		√

Note: A0 denotes the baseline scheme; A1 denotes single-measure schemes; A2 denotes combined-measure schemes; G denotes additional groundwater supply; D denotes water supplementation from the Eastern and Central Routes of the South-to-North Water Diversion Project; R denotes supplementation from the Longyangxia Reservoir; and the suffixes in R3-1, R5-1, and R5-2 indicate the scale of in-channel water supplementation.

3 | Methodology

3.1 | Quantitative Assessment Method for Water Supply–Demand Imbalance

Water supply–demand imbalance can generate economic losses across agricultural, industrial, domestic, and ecological sectors, while conventional deterministic estimates generally rely on water-shortage volume and the unit economic value of water. Meanwhile, the sensitivity to water shortage and the economic value of water vary substantially among water-use sectors, while realized water supply remains uncertain under severe low-flow conditions. Therefore, a single deterministic loss estimate based on a prescribed water-supply state may not adequately characterize the expected economic consequences of water supply–demand imbalance. Accordingly, this study develops an expected-risk assessment framework that combines a risk loss integral model with Monte Carlo simulation to quantify economic losses under uncertain water-supply conditions.

3.1.1 | Risk Loss Integral Model for Water Supply–Demand Imbalance

The formation of the economic impacts of water supply–demand imbalance can be regarded as a feedback process of risk exposure. Insufficient water supply may not immediately cause observable economic losses; however, when the shortage risk exceeds the tolerance capacity of the system, potential risk is transformed into actual economic loss. Accordingly, the risk of water supply–demand shortage is regarded as a potential loss, and a multiple integral model for water shortage risk is defined.

Let x denote water supply and y denote water demand. Parameters a and b represent the minimum and maximum values of water supply, respectively, while c and d represent the minimum and maximum values of water demand. Let $f(x,y)$ be the joint probability density function of water supply and water demand, and let $C(y-x)$ be the economic loss function under water-shortage conditions. The expected risk loss caused by water supply–demand imbalance can then be expressed as:

$$R_w = \int_a^b \int_c^d f(x,y)C(y-x)I_{(x<y)}\,dy\,dx \tag{1}$$

where R_w denotes the expected risk loss caused by water supply–demand imbalance, and $I_{(x<y)}$ is an indicator function that takes the value of 1 when $x < y$. Equation (1) indicates that water-shortage losses are calculated only when water supply is lower than water demand. In this way, the occurrence probability of water supply–demand imbalance and the corresponding loss severity are incorporated into a unified integral framework.

3.1.2 | Risk Loss Function for Water Supply–Demand Imbalance

For the economic impacts of regional water supply–demand imbalance, this study mainly considers the water-shortage losses that occur when water supply is lower than water demand. For quantitative estimation, the economic loss caused by water shortage is expressed as the product of the water shortage volume and the unit economic value of water:

$$C(y-x) = g(y-x) \tag{2}$$

where g denotes the unit economic value of water. By substituting Equation (2) into Equations (1) and (2), assumes a linear sector-specific relationship between water shortage volume and economic loss. The risk-based feature of the framework arises from integrating this loss function over alternative stochastic water-supply states subject to the shortage threshold, rather than from assuming a nonlinear marginal loss function. The expected risk expression for the economic losses caused by water supply–demand imbalance can be obtained as:

$$E_L = R_w = \int_a^b \int_c^d g(y-x)f(x,y)I_{(x<y)}\,dx\,dy \tag{3}$$

Regional water demand is commonly estimated using methods such as the quota method, which is related to factors including population, agricultural area, and water-use quotas. Therefore, under different water supply conditions, water demand is generally assumed to remain unchanged. In other words, the effects of changes in water-right allocation, agricultural structure, or inflow-year conditions on calculated water demand are considered negligible. In this case, the probability density function of water demand cannot adequately represent the distribution of water demand y_0. Accordingly, Equation (3) can be further transformed into a conditional expectation form under a fixed water demand condition:

$$E_L(y_0) = \int_a^{y_0} g \cdot (y_0 - x) f(x|y_0)\,dx \tag{4}$$

where $f(x|y_0)$ denotes the probability density function of water supply under the given water demand scenario. In the numerical implementation, this distribution is represented through Monte Carlo sampling around the scenario-specific target water supply. Equation (4) indicates that, under a specific water demand scenario, the economic losses caused by water supply–demand imbalance are determined by the occurrence probabilities of different water supply states and their corresponding water shortage volumes.

In the numerical simulation, Equation (4) is estimated using the Monte Carlo method for computational convenience. Assuming that N water supply samples $x_i (i = 1, 2, \cdots, N)$ are randomly generated under a given scenario, the economic losses caused by water supply–demand imbalance can be approximated as:

$$L_{\text{mon}}(y_0) = \frac{1}{N}\sum_{i=1}^{N} g(y_0 - x_i) I_{(x_i<y_0)} \tag{5}$$

where $L_{\text{mon}}(y_0)$ denotes the Monte Carlo estimated economic loss under the water demand scenario. For the i-th province under the k-th scenario, losses are calculated separately for the agricultural, industrial, domestic, and ecological water-use sectors, and the total loss is expressed as:

$$L_i^k = \frac{1}{N}\sum_{n=1}^{N}\sum_{m=1}^{M} g_{i,m}\left(y_{i,m}^k - x_{i,m,n}^k\right) I_{\left(x_{i,m,n}^k < y_{i,m}^k\right)} \quad (6)$$

where L_i^k denotes the economic loss caused by water supply–demand imbalance in the i-th province under the k-th scenario; M is the number of water-use sectors; $g_{i,m}$ represents the unit economic value of water for the m-th water-use sector in the i-th province; $y_{i,m}^k$ is the corresponding water demand; and $x_{i,m,n}^k$ denotes the water supply in the n-th simulation. The total economic loss in the Yellow River Basin is obtained by summing the losses across all provinces. Accordingly, the economic loss function for water supply–demand imbalance is expressed as:

$$L^k = \sum_{i=1}^{I} L_i^k \quad (7)$$

where L^k denotes the total economic loss caused by water supply–demand imbalance in the Yellow River Basin under the k-th scenario, and I is the number of provinces.

3.2 | Economic Loss Assessment of Water Supply–Demand Imbalance

Based on the established risk loss function for water supply–demand imbalance, the loss function is combined with severe low-flow scenarios to construct a quantitative model for assessing the economic losses caused by water supply–demand imbalance in the Yellow River Basin. The specific procedures are as follows:

1. Identification of low-flow scenarios

Different inflow-year types in the study area are defined, and typical low-flow years, consecutive low-flow periods, and multi-scheme regulation scenarios for a severe low-flow year are determined. These scenarios provide the basis for subsequent water supply–demand analysis and loss calculation.

2. Analysis of water supply scenarios

Based on the current water supply structure of the study area, including surface water, groundwater, inter-basin transferred water, and non-conventional water, the water-supply constraints under different scenarios are identified. Differences in water-source structures among provinces are further examined to provide a basis for simulating water supply allocation under severe low-flow scenarios.

3. Generation of random water supply samples

For each low-flow scenario, the sectoral water allocation determined under the corresponding scenario is taken as the target water-supply level. To account for uncertainty in realized water supply arising from reservoir operation, water allocation, and other operational factors, Monte Carlo simulation is performed by introducing a dimensionless disturbance coefficient around the target allocation. For province i, water-use sector j, and scenario k, the water supply in the m-th simulation is expressed as

$$S_{ijk}^m = S_{ijk}^0\left(1 + \varepsilon_{ijk}^m\right) \quad (8)$$

where S_{ijk}^0 denotes the scenario-specific target water supply and ε_{ijk}^m denotes the random disturbance coefficient. The disturbance coefficient is assumed to follow a uniform distribution over the interval (−0.03, 0.03), corresponding to an allowable fluctuation of ±3% around the target allocation. A uniform distribution is adopted because insufficient empirical evidence is available to assign different occurrence probabilities to individual supply states within this relatively narrow operational range.

To maintain consistency with the total water availability prescribed for each low-flow scenario, the randomly generated sectoral supplies are further constrained by the scenario-specific total water supply. If the relative deviation between the sampled total supply and the prescribed total supply exceeds 3%, the sample is rejected and regenerated, followed by total-volume calibration where necessary. A total of 10,000 Monte Carlo realizations are generated for each scenario and used to estimate the expected economic loss. The stochastic simulation therefore represents uncertainty in realized water supply conditional on a prescribed low-flow scenario, rather than the probability of occurrence of the low-flow scenario itself.

4. Determination of the unit economic value of water

The quantification of economic losses depends on the unit economic value of water (g, CNY/m^3) for different water-use sectors. In this study, the values of g for the agricultural, industrial, domestic, and ecological sectors were determined with reference to Wu et al. (2020), who evaluated the spatial differences in water-use value across provinces in the Yellow River Basin. Province-specific values were adopted rather than a uniform basin-wide coefficient so that regional differences in economic development and water-use efficiency could be retained in the loss assessment. These sector- and province-specific values were subsequently used as the basic parameters in Equations (5–7).

4 | Results and Discussion

4.1 | Economic Losses Under Typical Low-Flow Year Scenarios

1. Current condition in 2022

Under the 2022 condition, economic losses increase markedly with the severity of low-flow conditions (Figure 2). Under the 75% inflow-frequency scenario, the basin-wide loss is 74.66×10^8 CNY and occurs only in Inner Mongolia (53.09×10^8 CNY) and Ningxia (21.57×10^8 CNY). Under the 90% scenario, the total loss increases to 128.00×10^8 CNY, with losses of 92.90×10^8 CNY and 35.10×10^8 CNY in Inner Mongolia and Ningxia, respectively. Under the 95% scenario, the total loss reaches 574.82×10^8 CNY and expands to five provinces, including Inner Mongolia (253.00×10^8 CNY), Ningxia (89.53×10^8 CNY), Gansu (40.11×10^8 CNY), Shaanxi (192.01×10^8 CNY), and Sichuan (0.17×10^8 CNY). No economic losses are observed in Qinghai, Shanxi, Henan, or Shandong.

The spatial differences are consistent with the provincial water-use and water-supply structures. In 2022, agricultural

water use accounted for 80.9%, 66.5%, and 63.6% of total water use in Ningxia, Inner Mongolia, and Gansu, respectively, while surface water accounted for 90.6%, 72.6%, and 86.7% of their total supply. Under the 95% scenario, these three provinces alone accounted for 66.6% of the basin-wide economic loss. By comparison, non-surface water sources accounted for 46.2% of total supply in Henan and 51.7% in Shandong, where no economic losses occurred under the same scenario. These contrasts indicate that the spatial distribution of losses is closely associated with regional differences in water-use structure and alternative water-supply capacity.

2. Planned condition in 2035

Under the 2035 planned condition, economic losses are generally higher and affect more provinces than under the 2022 condition (Figure 3). The basin-wide losses under the 75%, 90%, and 95% inflow-frequency scenarios are 264.11×10^8 CNY, 346.69×10^8 CNY, and 730.19×10^8 CNY, respectively. Under the 95% scenario, losses occur in eight provinces: Inner Mongolia (208.17×10^8 CNY), Ningxia (78.38×10^8 CNY), Gansu (72.69×10^8 CNY), Qinghai (35.83×10^8 CNY), Shaanxi (105.85×10^8 CNY), Shanxi (154.18×10^8 CNY), Henan (74.46×10^8 CNY), and Sichuan (0.63×10^8 CNY), while no loss occurs in Shandong. A sensitivity test was further conducted for the 95% inflow-frequency scenario under the 2022 condition by replacing the uniform distribution with a triangular distribution while retaining the same ±3% fluctuation range and 10,000 sampling runs. The basin-wide economic loss changed only slightly, and the spatial pattern of high-loss provinces remained unchanged. This indicates that the principal assessment results are not sensitive to the choice between

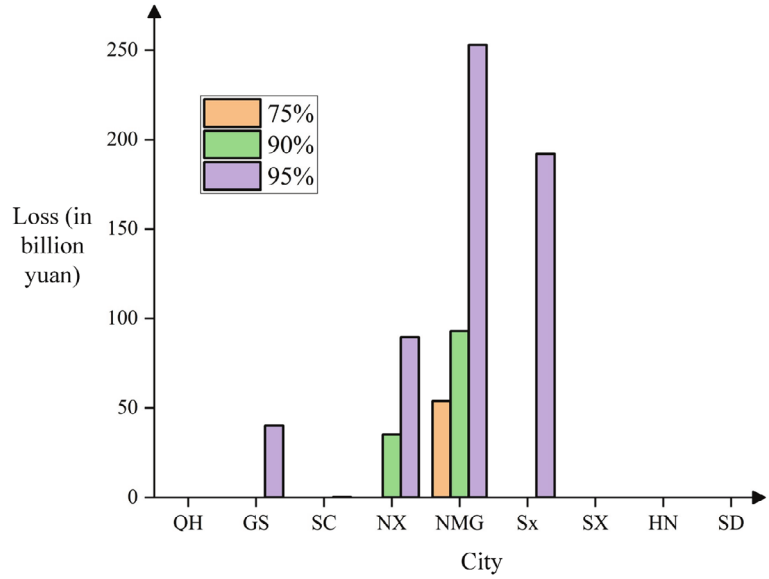

FIGURE 2 | Economic losses caused by water supply–demand imbalance under different inflow-frequency scenarios in 2022.

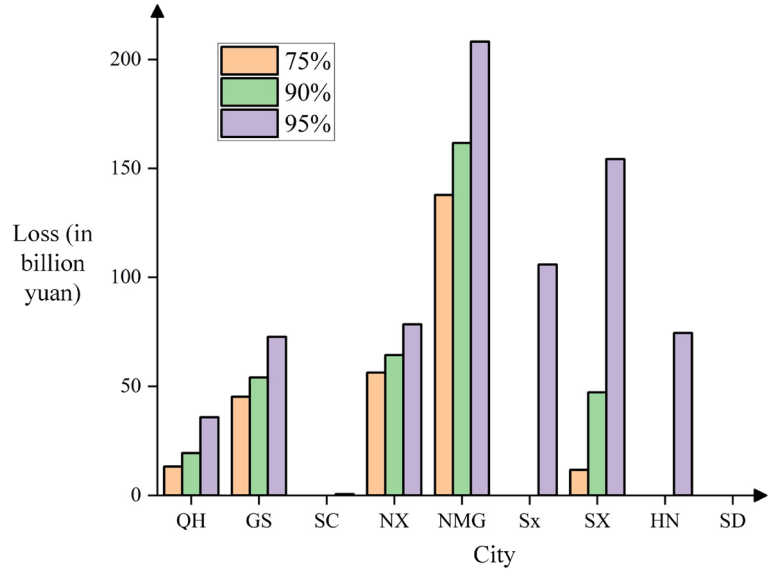

FIGURE 3 | Economic losses caused by water supply–demand imbalance under different inflow-frequency scenarios in 2035.

the two sampling distributions within the prescribed fluctuation range.

Under the planned condition, the overall loss magnitude is higher than that under the current condition, indicating greater economic exposure under the same low-flow conditions. Under the 75% and 90% inflow-frequency scenarios, the affected area expands from only two provinces under the current condition to more provinces in the middle and upper reaches. Under the 95% inflow-frequency scenario, Inner Mongolia remains the core high-loss area, while more pronounced increases in losses are observed in Shanxi, Shaanxi, and Henan. This can be attributed to the increase in total water demand, the strengthening of water-use rigidity, the continued large shares of agricultural and industrial water demand, and the limited compensation capacity of alternative water sources and regulation measures under the planned condition. Consequently, low-flow shocks are transformed into economic losses over a broader spatial extent.

4.2 | Economic Losses Under Consecutive Low-Flow Period Scenarios

1. Current condition in 2022

When the consecutive low-flow period from 1990 to 2002 is imposed under the 2022 condition, economic losses show a clear temporal accumulation pattern, characterized by low values in the early stage, gradual increases in the middle stage, and rapid growth in the later stage (Figure 4). In 1991, losses occur only in Ningxia and Inner Mongolia, reaching 39.0×10^8 CNY and 104.2×10^8 CNY, respectively. By 1997, losses expand to four provinces, reaching 65.9×10^8 CNY in Ningxia, 183.4×10^8 CNY in Inner Mongolia, 13.9×10^8 CNY in Gansu, and 72.5×10^8 CNY in Shaanxi. In 2002, the losses further increase to 253.0×10^8 CNY in Inner Mongolia, 89.5×10^8 CNY in Ningxia, 192.0×10^8 CNY in Shaanxi, 40.1×10^8 CNY in Gansu, and 0.2×10^8 CNY in Sichuan.

Overall, losses progressively expand from a few provinces to a broader area in the middle and upper reaches. The persistent concentration of high losses in Inner Mongolia, Ningxia, Gansu, and Shaanxi is consistent with their relatively high agricultural water demand, stronger constraints on surface-water supply, and limited alternative water-source regulation capacity. Thus, prolonged low inflow not only increases loss magnitude but also enlarges the spatial extent of water supply–demand imbalance.

2. Planned condition in 2035

Under the 2035 planned condition, the temporal pattern remains broadly consistent with that in 2022, with relatively stable losses in the early stage, increasing losses in the middle stage, and stronger accumulation in the later stage (Figure 5). The years 1997, 2001, and 2002 are identified as major high-loss years, with losses in Inner Mongolia exceeding 170×10^8 CNY in each year; relatively high losses also occur in Gansu, Ningxia, and Shaanxi.

Compared with the 2022 condition, the overall loss magnitude is higher and the affected area is broader under the 2035 scenario. This pattern suggests that higher planned water demand increases the basin's exposure to persistent low inflow, while the existing water-use structure and limited alternative water-supply capacity in the middle and upper reaches further constrain system adjustment. Consequently, consecutive low-flow events impose greater economic pressure under the planned condition.

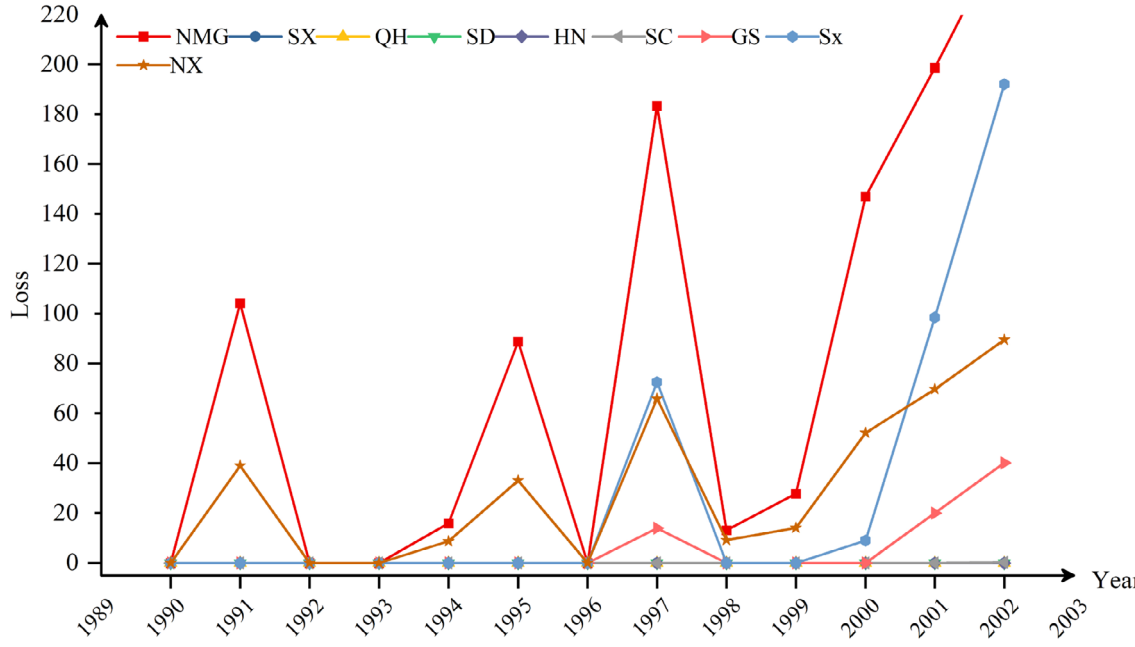

FIGURE 4 | Economic losses caused by water supply–demand imbalance during the consecutive low-flow period under the 2022 current condition.

4.3 | Economic Losses Under Multi-Scheme Regulation Scenarios for a Severe Low-Flow Year

1. Current condition in 2022

When the severe low-flow year of 2002 is imposed under the 2022 condition, economic losses generally decrease with increasing supplementary water supply across the 16 regulation schemes (Figure 6). The A0 scheme without regulation produces the highest loss, reaching 575×10^8 CNY. Under the single-measure schemes, losses range from 268×10^8 CNY to 487×10^8 CNY, indicating that groundwater supplementation, water diversion, reservoir regulation, and in-channel supplementation can all reduce losses to different degrees. Increasing reservoir supplementation also generally reduces the loss, although the magnitude of reduction varies among supplementation levels.

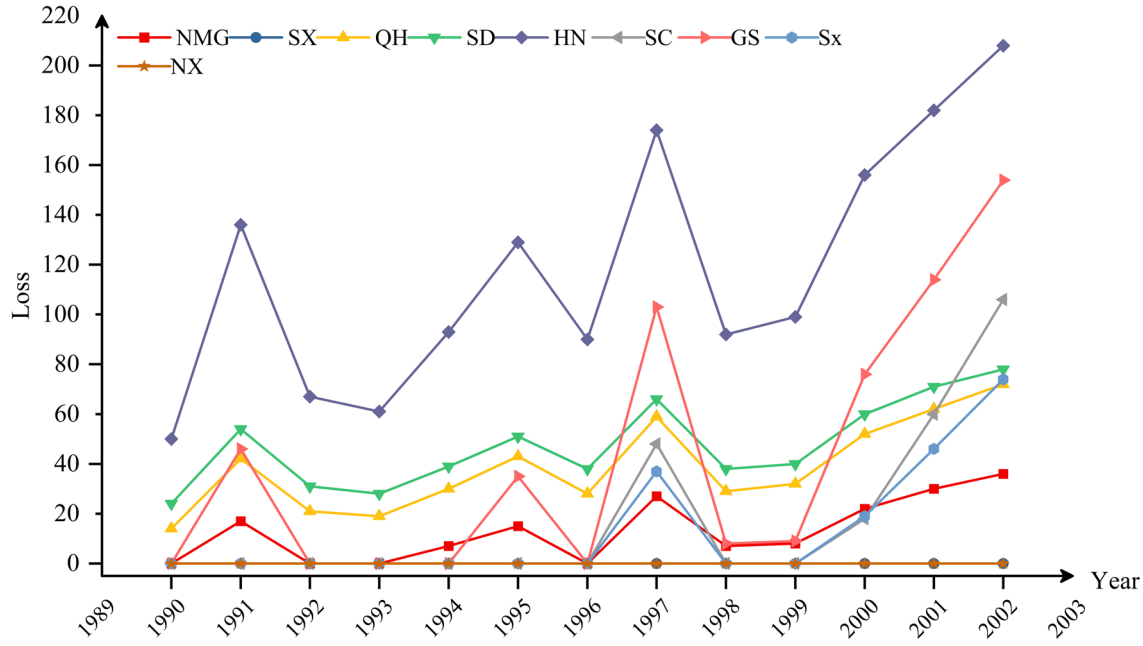

FIGURE 5 | Economic losses caused by water supply–demand imbalance during the consecutive low-flow period under the 2035 planned condition.

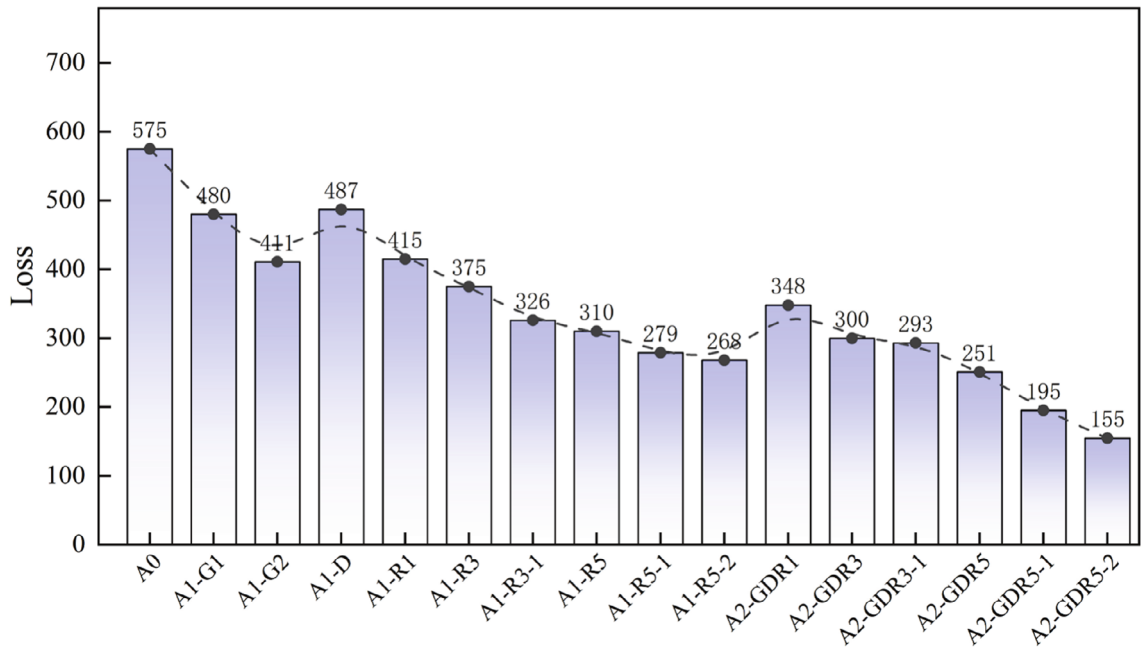

FIGURE 6 | Economic losses caused by water supply–demand imbalance under different regulation schemes for the severe low-flow year under the 2022 current condition.

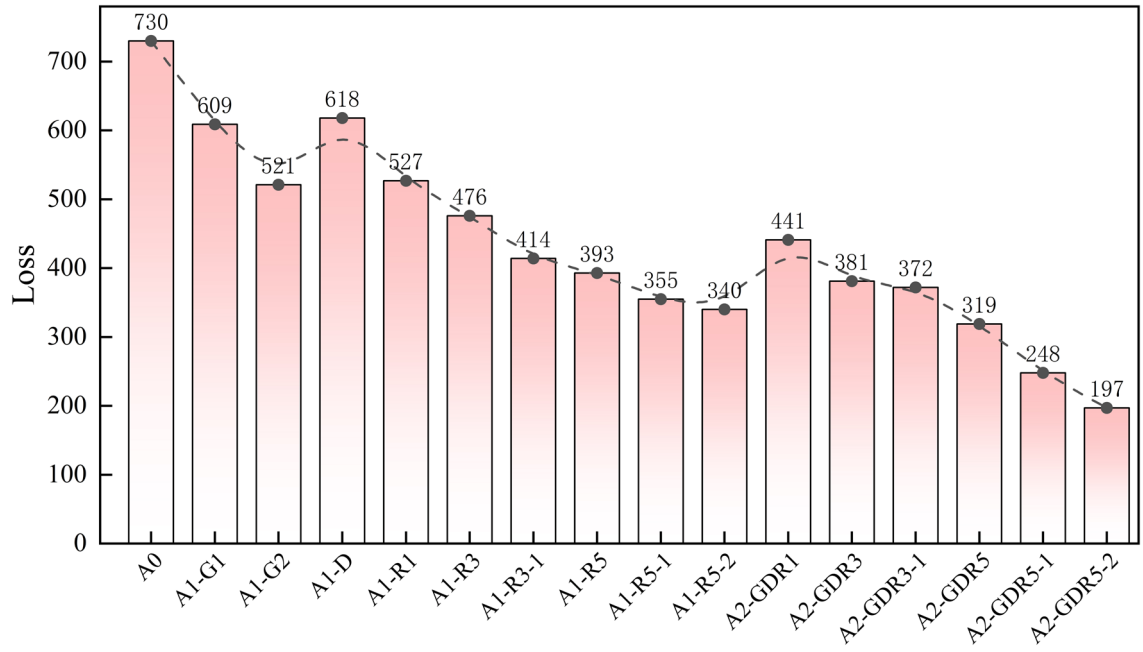

FIGURE 7 | Economic losses caused by water supply–demand imbalance under different regulation schemes for the severe low-flow year under the 2035 planned condition.

Combined regulation provides a stronger overall loss-reduction effect. Losses under the A2-GDR series range from 155×10^8 CNY to 348×10^8 CNY, lower overall than those under the single-measure schemes. Under A2-GDR5-2, the loss decreases from 575×10^8 CNY to 155×10^8 CNY, corresponding to a reduction of approximately 73.0%. This comparison demonstrates the greater effectiveness of coordinated multi-source regulation under severe low-flow conditions.

2. Planned condition in 2035

Under the 2035 planned condition, economic losses show a similar response to regulation, but remain generally higher than under the 2022 condition (Figure 7). The loss under A0 reaches 730×10^8 CNY. Losses under the single-measure schemes range from 340×10^8 CNY to 618×10^8 CNY, whereas those under the combined schemes range from 197×10^8 CNY to 441×10^8 CNY. Under A2-GDR5-2, the loss decreases to 197×10^8 CNY, representing a reduction of approximately 73.0% relative to A0. Overall, the results show that combined regulation maintains substantial loss-reduction capacity even under the higher planned water-demand condition. The consistently lower losses under combined schemes indicate that coordination among multiple water sources provides greater flexibility for mitigating water supply–demand imbalance than reliance on a single supplementary pathway.

A sensitivity analysis was conducted using the 2022 condition under the 95% inflow-frequency scenario as a representative case. Water demand and the unit economic value of water (g) varied by 10% around their baseline values to examine their effects on the estimated economic loss. Water-supply uncertainty was further tested by replacing the uniform distribution with a triangular distribution while retaining the same ±3% fluctuation range and 10,000 Monte Carlo runs. In addition, the sensitivity to regulation quantity was examined through the existing low-, medium-, and high-supplementation schemes in Table 3. The results showed that changes in these parameters affected the magnitude of the estimated losses, but the overall spatial pattern and the relative differences among scenarios remained generally stable, indicating that the main conclusions are robust to reasonable variations in the key model assumptions.

Several sources of uncertainty should be considered when interpreting the results. In addition to stochastic water supply, the 2035 water-demand scenario is subject to uncertainties in future socioeconomic development, water-use efficiency, and planning assumptions. The estimated water demand and sector-specific unit economic values may also vary with data sources and temporal changes. Therefore, the calculated losses should be interpreted primarily as comparative estimates among scenarios rather than exact predictions of future economic damage. Future studies could incorporate dynamic water-demand responses and time-varying economic value parameters to further improve the framework.

5 | Conclusion

An economic loss assessment framework for water supply–demand imbalance in the Yellow River Basin under severe low-flow scenarios was developed in this study. A risk loss integral model and Monte Carlo simulation were used to quantitatively analyze economic losses under typical low-flow year scenarios, consecutive low-flow period scenarios, and multi-scheme regulation scenarios for a severe low-flow year. The results show that economic losses in the Yellow River Basin increase markedly as inflow conditions deteriorate, and the affected areas expand from a few local provinces to the middle and upper reaches. Under the 2022 current condition, the total basin-wide economic losses corresponding to the 75%,

90%, and 95% inflow-frequency scenarios are 74.66×10^8 CNY, 128.00×10^8 CNY, and 574.82×10^8 CNY, respectively. Under the 2035 planned condition, the corresponding losses increase to 264.11×10^8 CNY, 346.69×10^8 CNY, and 730.19×10^8 CNY, respectively. The analysis of the consecutive low-flow period indicates that economic losses show a clear cumulative pattern during the persistently dry period from 1990 to 2002, with relatively low losses in the early stage, a gradual increase in the middle stage, and a rapid rise in the later stage. Inner Mongolia, Ningxia, Gansu, and Shaanxi are identified as the major high-loss areas under both typical low-flow year and consecutive low-flow period scenarios, indicating that the high proportion of agricultural water use, strong dependence on surface water, and limited alternative water-source capacity in the middle and upper reaches continuously amplify the risk of water supply–demand imbalance under low-flow conditions.

The multi-scheme regulation analysis for the severe low-flow year shows that different supplementary water-supply measures can all reduce the economic losses caused by water supply–demand imbalance, and the loss-reduction effects of combined regulation schemes are generally greater than those of single-measure schemes. Under the 2022 current condition, the loss under the A0 scheme is 575×10^8 CNY, while the A2-GDR5-2 scheme reduces the loss to approximately 155×10^8 CNY. Under the 2035 planned condition, the corresponding losses are 730×10^8 CNY and 197×10^8 CNY, respectively, indicating that coordinated multi-source water allocation still has strong loss-reduction capacity under future water-demand growth. The response of losses to regulation measures exhibits nonlinear characteristics. Although increasing the scale of supplementary water supply can further reduce losses, the marginal loss-reduction effect gradually weakens. These results suggest that the response to low-flow risks in the Yellow River Basin should not rely on a single supplementary water-supply pathway. Instead, stronger coordination should be promoted among groundwater supplementation, reservoir supplementation, inter-basin water diversion, and demand-side management. In this study, water demand is treated as fixed within each scenario, and a linear loss function based on the unit economic value of water is used to characterize sectoral losses. Therefore, the nonlinear evolution of water-use reduction, structural adjustment, and ecological losses has not yet been fully represented. Future studies could incorporate dynamic water-demand responses and nonlinear loss functions to further improve the explanatory capacity and decision-support value of economic loss assessment under severe low-flow conditions.

Author Contributions

Wenxiu Shang: conceptualization, methodology, writing – review and editing, writing – original draft, formal analysis, funding acquisition. **Juan Jing:** data curation, methodology, investigation. **Yifan Wei:** methodology, formal analysis. **Haodong Deng:** validation, writing – review and editing, formal analysis, resources. **Hong Lv:** formal analysis, data curation, software. **Xiaokang Zheng:** project administration, resources.

Funding

This research was funded by the National Natural Science Foundation of China (U2243233 and 52509039).

Conflicts of Interest

The authors declare no conflicts of interest.

Data Availability Statement

The data that support the findings of this study are available on request from the corresponding author. The data are not publicly available due to privacy or ethical restrictions.

References

AghaKouchak, A., A. Mirchi, K. Madani, et al. 2021. "Anthropogenic Drought: Definition, Challenges, and Opportunities." *Reviews of Geophysics* 59: e2019RG000683. https://doi.org/10.1029/2019RG000683.

Beven, K., and A. Binley. 1992. "The Future of Distributed Models: Model Calibration and Uncertainty Prediction." *Hydrological Processes* 6, no. 3: 279–298. https://doi.org/10.1002/hyp.3360060305.

Cai, X., D. C. McKinney, and M. W. Rosegrant. 2004. "Optimal Water Development Strategies for the Yellow River Basin: Balancing Agricultural and Ecological Water Demands." *Water Resources Research* 40: W08S04. https://doi.org/10.1029/2003WR002488.

Dai, A. 2013. "Increasing Drought Under Global Warming in Observations and Models." *Nature Climate Change* 3: 52–58. https://doi.org/10.1038/nclimate1633.

Di Baldassarre, G., N. Wanders, A. AghaKouchak, et al. 2018. "Water Shortages Worsened by Reservoir Effects." *Nature Sustainability* 1: 617–622. https://doi.org/10.1038/s41893-018-0159-0.

Fleming-Muñoz, D. A., S. Whitten, and G. D. Bonnett. 2023. "The Economics of Drought: A Review of Impacts and Costs." *Australian Journal of Agricultural and Resource Economics* 67, no. 4: 501–523. https://doi.org/10.1111/1467-8489.12527.

Flörke, M., C. Schneider, and R. I. McDonald. 2018. "Water Competition Between Cities and Agriculture Driven by Climate Change and Urban Growth." *Nature Sustainability* 1: 51–58. https://doi.org/10.1038/s41893-017-0006-8.

Freire-González, J., C. Decker, and J. W. Hall. 2017. "The Economic Impacts of Droughts: A Framework for Analysis." *Ecological Economics* 132: 196–204. https://doi.org/10.1016/j.ecolecon.2016.11.005.

Haddeland, I., J. Heinke, H. Biemans, et al. 2014. "Global Water Resources Affected by Human Interventions and Climate Change." *Proceedings of the National Academy of Sciences of the United States of America* 111, no. 9: 3251–3256. https://doi.org/10.1073/pnas.1222475110.

Hanasaki, N., S. Fujimori, T. Yamamoto, et al. 2013. "A Global Water Scarcity Assessment Under Shared Socio-Economic Pathways. Part 2: Water Availability and Scarcity." *Hydrology and Earth System Sciences* 17: 2393–2413. https://doi.org/10.5194/hess-17-2393-2013.

Hashimoto, T., J. R. Stedinger, and D. P. Loucks. 1982. "Reliability, Resiliency, and Vulnerability Criteria for Water Resource System Performance Evaluation." *Water Resources Research* 18, no. 1: 14–20. https://doi.org/10.1029/WR018i001p00014.

Hoekstra, A. Y., M. M. Mekonnen, A. K. Chapagain, R. E. Mathews, and B. D. Richter. 2012. "Global Monthly Water Scarcity: Blue Water Footprints Versus Blue Water Availability." *PLoS One* 7, no. 2: e32688. https://doi.org/10.1371/journal.pone.0032688.

Hu, L., Y. Xie, Y. Liu, et al. 2025. "Mapping the Primary Factors Driving Spatiotemporal Variations of Surface Soil Moisture in the Yellow River Basin of China." *Scientific Reports* 15: 12359. https://doi.org/10.1038/s41598-025-96129-w.

Jenkins, K., B. Dobson, C. Decker, and J. W. Hall. 2021. "An Integrated Framework for Risk-Based Analysis of Economic Impacts of Drought

and Water Scarcity in England and Wales." *Water Resources Research* 57: e2020WR027715. https://doi.org/10.1029/2020WR027715.

Jiang, S., L. Zhou, L. Ren, et al. 2021. "Development of a Comprehensive Framework for Quantifying the Impacts of Climate Change and Human Activities on River Hydrological Health Variation." *Journal of Hydrology* 600: 126566. https://doi.org/10.1016/j.jhydrol.2021.126566.

Kuczera, G., and E. Parent. 1998. "Monte Carlo Assessment of Parameter Uncertainty in Conceptual Catchment Models: The Metropolis Algorithm." *Journal of Hydrology* 211, no. 1–4: 69–85. https://doi.org/10.1016/S0022-1694(98)00198-X.

Li, Z., S. Huang, Y. Wang, et al. 2026. "A Process-Oriented Framework to Decipher Drought Propagation Dynamics From Meteorological to Ecological, Agricultural, Hydrological, and Socioeconomic Drought in the Yellow River Basin." *Ecological Indicators* 182: 114574. https://doi.org/10.1016/j.ecolind.2025.114574.

Liu, J., H. Yang, S. N. Gosling, et al. 2017. "Water Scarcity Assessments in the Past, Present, and Future." *Earth's Future* 5, no. 6: 545–559. https://doi.org/10.1002/2016EF000518.

Logar, I., and J. C. J. M. van den Bergh. 2013. "Methods to Assess Costs of Drought Damages and Policies for Drought Mitigation and Adaptation: Review and Recommendations." *Water Resources Management* 27: 1707–1720. https://doi.org/10.1007/s11269-012-0119-9.

Mekonnen, M. M., and A. Y. Hoekstra. 2016. "Four Billion People Facing Severe Water Scarcity." *Science Advances* 2, no. 2: e1500323. https://doi.org/10.1126/sciadv.1500323.

Miao, C. Y., W. Shi, X. H. Chen, and L. Yang. 2012. "Spatio-Temporal Variability of Streamflow in the Yellow River: Possible Causes and Implications." *Hydrological Sciences Journal* 57, no. 7: 1355–1367. https://doi.org/10.1080/02626667.2012.718077.

Mishra, A. K., and V. P. Singh. 2010. "A Review of Drought Concepts." *Journal of Hydrology* 391, no. 1–2: 202–216. https://doi.org/10.1016/j.jhydrol.2010.07.012.

Mortazavi-Naeini, M., G. Bussi, J. A. Elliott, J. W. Hall, and P. G. Whitehead. 2019. "Assessment of Risks to Public Water Supply From Low Flows and Harmful Water Quality in a Changing Climate." *Water Resources Research* 55, no. 12: 10386–10404. https://doi.org/10.1029/2018WR022865.

Mukama, E. B., E. A. Yimer, W. B. Mbungu, S. Dondeyne, and A. van Griensven. 2025. "Evaluating the Standardized and Threshold-Based Drought Indices for Historical Drought Detection in the Great Ruaha River Basin, Tanzania." *Natural Hazards* 121: 12243–12273. https://doi.org/10.1007/s11069-025-07279-z.

Piao, S., P. Ciais, Y. Huang, et al. 2010. "The Impacts of Climate Change on Water Resources and Agriculture in China." *Nature* 467: 43–51. https://doi.org/10.1038/nature09364.

Salmoral, G., D. Rey, A. Rudd, P. de Margon, and I. P. Holman. 2019. "A Probabilistic Risk Assessment of the National Economic Impacts of Regulatory Drought Management on Irrigated Agriculture." *Earth's Future* 7, no. 2: 178–196. https://doi.org/10.1029/2018EF001092.

Schewe, J., J. Heinke, D. Gerten, et al. 2014. "Multimodel Assessment of Water Scarcity Under Climate Change." *Proceedings of the National Academy of Sciences of the United States of America* 111, no. 9: 3245–3250. https://doi.org/10.1073/pnas.1222460110.

Stahl, K., I. Kohn, V. Blauhut, et al. 2016. "Impacts of European Drought Events: Insights From an International Impact Report Inventory." *Natural Hazards and Earth System Sciences* 16: 801–819. https://doi.org/10.5194/nhess-16-801-2016.

Trenberth, K. E., A. Dai, G. van der Schrier, et al. 2014. "Global Warming and Changes in Drought." *Nature Climate Change* 4: 17–22. https://doi.org/10.1038/nclimate2067.

Van Loon, A. F. 2015. "Hydrological Drought Explained." *WIREs Water* 2, no. 4: 359–392. https://doi.org/10.1002/wat2.1085.

Van Loon, A. F., T. Gleeson, J. Clark, et al. 2016. "Drought in the Anthropocene." *Nature Geoscience* 9: 89–91. https://doi.org/10.1038/ngeo2646.

Vörösmarty, C. J., P. Green, J. Salisbury, and R. B. Lammers. 2000. "Global Water Resources: Vulnerability From Climate Change and Population Growth." *Science* 289, no. 5477: 284–288. https://doi.org/10.1126/science.289.5477.284.

Wanders, N., and Y. Wada. 2015. "Human and Climate Impacts on the 21st Century Hydrological Drought." *Journal of Hydrology* 526: 208–220. https://doi.org/10.1016/j.jhydrol.2014.10.047.

Wang, L., Y. Li, A. Biswas, Y. Zhao, B. Niu, and K. H. M. Siddique. 2025. "Assessing Climate Change and Human Impacts on Runoff and Hydrological Droughts in the Yellow River Basin Using a Machine Learning-Enhanced Hydrological Modeling Approach." *Journal of Environmental Management* 380: 125091. https://doi.org/10.1016/j.jenvman.2025.125091.

Wang, Y., Y. Ding, B. Ye, F. Liu, and J. Wang. 2013. "Contributions of Climate and Human Activities to Changes in Runoff of the Yellow and Yangtze Rivers From 1950 to 2008." *Science China Earth Sciences* 56: 1398–1412. https://doi.org/10.1007/s11430-012-4505-1.

Wang, Y., X. K. Zheng, H. Lv, et al. 2025. "Resilience Regulation of Water Resources System in the Yellow River Basin During Extreme Low-Flow Years." *Advances in Water Science* 36, no. 3: 359–371. (in Chinese). https://doi.org/10.14042/j.cnki.32.1309.2025.03.001.

Wu, J., H. Yao, P. An, et al. 2026. "Propagation Patterns of Hydrological Droughts in the Source Region of Yellow River: Insights From Standardized Versus Threshold-Based Approaches." *River* 5: 55–68. https://doi.org/10.1002/rvr2.70039.

Wu, Z., D. Di, and S. Huang. 2020. "Analysis of Spatial Clustering Characteristics of Water Resources Value in Each Region of the Yellow River Basin." *Yellow River* 42: 96–100. (in Chinese). https://doi.org/10.3969/i.issn.1000-1379.2020.09.018.

Yang, L., G. Zhao, P. Tian, et al. 2022. "Runoff Changes in the Major River Basins of China and Their Responses to Potential Driving Forces." *Journal of Hydrology* 607: 127536. https://doi.org/10.1016/j.jhydrol.2022.127536.

Yang, M., X. Li, K. Song, et al. 2026. "Multi-Source Joint Water Allocation and Route Interconnection Under Low-Flow Conditions: An IMWA-IRRS Framework for the Yellow River Water Supply Region Within Water Network Layout." *Sustainability* 18, no. 3: 1541. https://doi.org/10.3390/su18031541.

Yang, X., X. Liao, D. Di, and W. Shi. 2023. "A Review of Drought Disturbance on Socioeconomic Development." *Water* 15, no. 22: 3912. https://doi.org/10.3390/w15223912.

Zhen, N., R. Yao, P. Sun, Q. Zhang, C. Ge, and H. Shen. 2025. "Triggering Thresholds and Influential Factors in the Propagation of Meteorological Drought to Hydrological Drought." *Journal of Hydrology: Regional Studies* 57: 102184. https://doi.org/10.1016/j.ejrh.2025.102184.